Processing and properties of eco-friendly bio-nanocomposite films filled with cellulose nanocrystals from sugarcane bagasse

Mounir El Achaby, Nassima El Miri, Adil Aboulkas, Mohamed Zahouily, Essaïd Bilal, Abdellatif Barakat, Abderrahim Solhy

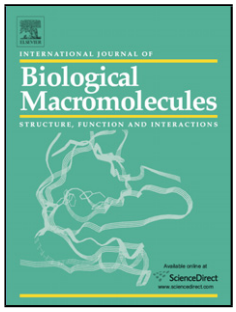

Title: Processing and Properties of Eco-friendly Bio-nanocomposite Films Filled with Cellulose Nanocrystals from Sugarcane Bagasse

Author: Mounir El Achaby Nassima El Miri Adil Aboulkas Mohamed Zahouily Bilal Essaid Abdellatif Barakat Abderrahim Solhy

PII: S0141-8130(16)31519-7
DOI: http://dx.doi.org/doi:10.1016/j.ijbiomac.2016.12.040
Reference: BIOMAC 6855

To appear in: *International Journal of Biological Macromolecules*

Received date: 5-9-2016
Revised date: 21-11-2016
Accepted date: 7-12-2016

Please cite this article as: Mounir El Achaby, Nassima El Miri, Adil Aboulkas, Mohamed Zahouily, Bilal Essaid, Abdellatif Barakat, Abderrahim Solhy, Processing and Properties of Eco-friendly Bio-nanocomposite Films Filled with Cellulose Nanocrystals from Sugarcane Bagasse, International Journal of Biological Macromolecules http://dx.doi.org/10.1016/j.ijbiomac.2016.12.040

Processing and Properties of Eco-friendly Bio-nanocomposite Films Filled with Cellulose Nanocrystals from Sugarcane Bagasse

Mounir El Achaby,[a,*] Nassima El Miri,[b] Adil Aboulkas,[c] Mohamed Zahouily[b], Bilal Essaid,[d] Abdellatif Barakat,[e] and Abderrahim Solhy,[a]

[a] Center for Advanced Materials, Mohammed VI Polytechnic University, Lot 660-Hay Moulay Rachid, 43150 Benguerir, Morocco

[b] Moroccan Foundation for Advanced Science Innovation and Research (MAScIR), Rabat Design, Rue Mohamed El Jazouli, Madinat El Irfane 10100-Rabat, Morocco

[c] Laboratoire Interdisciplinaire de Recherche en Sciences et Techniques, Faculté polydisciplinaire de Béni-Mellal, Université Sultan Moulay Slimane, BP 592, 23000 Béni-Mellal, Morocco

[d] R&D OCP, OCP Group, Complexe industriel Jorf Lasfar. BP 118 El Jadida, Morocco

[e] IATE, CIRAD, Montpellier SupAgro, INRA, Université de Montpelier, 34060, Montpellier, France

[*]Corresponding author. Tel: (+212)662010620; E-mail addresses: mounir.elachaby@um6p.ma (M. El Achaby)

Abstract

Novel synthesis strategy of eco-friendly bio-nanocomposite films have been exploited using cellulose nanocrystals (CNC) and polyvinyl alcohol/carboxymethyl cellulose (PVA/CMC) blend matrix as a potential in food packaging application. The CNC were extracted from sugarcane bagasse using sulfuric acid hydrolysis, and they were successfully characterized regarding their morphology, size, crystallinity and thermal stability. Thereafter, PVA/CMC-CNC bio-nanocomposite films, at various CNC contents (0.5-10 wt%), were fabricated by the solvent casting method, and their properties were investigated. It was found that the addition of 5 wt % CNC within a PVA/CMC increased the tensile modulus and strength by 141 % and 83 % respectively, and the water vapor permeability was reduced by 87 %. Additionally, the bio-nanocomposites maintained the same transparency level of the PVA/CMC blend film (transmittance of ~ 90 % in the visible region), suggesting that the CNC were dispersed at the nanoscale. In these bio-nanocomposites, the adhesion properties and the large number of functional groups that are present in the CNC's surface and the macromolecular chains of the PVA/CMC blend are exploited to improve the interfacial interactions between the CNC and the blend. Consequently, these eco-friendly structured bio-nanocomposites with superior properties are expected to be useful in food packaging applications.

Key words: Cellulose nanocrystals, Polymer blend, Bio-nanocomposite films.

1. Introduction

Recently, significant research has been devoted to the use of biopolymers owing to their advantages such as biodegradability, non-toxicity, availability, low cost, and potential wide range of applications, especially in the field of biomaterials and packaging applications [1,2]. Although biopolymers are considered potential replacements for conventional plastic materials, some of their properties must be improved to position them as materials that can be competitive with fossil derivatives, especially their poor mechanical, thermal, and barrier properties [3]. However, the blending of biopolymers and/or adding of nanofillers represents an effective way to improve the properties of biopolymers and, therefore, broadens their fields of application [1,4].

Blending of highly compatible biopolymers represent an effective way to develop new innovative biomaterials [5]. Due to the presence of strong intermolecular interactions, films produced from the blending of biopolymers usually exhibit improved properties as compared to films made from an individual biopolymer [6,7]. On the other hand, the processing of bio-nanocomposite materials with low loading of nanofillers has already been proven as an effective strategy to produce new nanostructured materials with innovative properties and high performances for packaging applications [1,4,8,9]. The incorporation of well-dispersed nanofillers into a polymeric matrix may result in improved physico-chemical properties of the resulting bio-nanocomposites, especially the mechanical, optical, thermal, and barrier properties [3,10-12].

Polyvinyl alcohol (PVA) and carboxymethyl cellulose (CMC) biopolymers have been widely used for development of biodegradable films for packaging applications [6,9]. The PVA and CMC are miscible and compatible biopolymers, due to the presence of multifunctional groups on their macromolecular chains [13-16]. Consequently, the blending

of these polymers can enable the preparation of biodegradable materials with properties that allow their application in the emerging field of bio-packaging [17,18]. More importantly, the PVA/CMC blend can be used as a new biocompatible and homogeneous blend matrix for bio-nanocomposite development to achieve high-performance packaging materials. Recently, elongated cellulose nanocrystals (CNC) for bio-nanocomposite development have attracted attention in the field of nanotechnology. These nanoparticles, which can be sphere-like, rod-like, ribbon-like, or needle-like, have a length ranging from 100 nm up to 1–2 mm, and a diameter of about 5–20 nm [3]. The main features that stimulate the use of CNC as polymer reinforcement agents are its large specific surface area (estimated to be several hundreds of square meters per gram) and its very high modulus of elasticity (approximately 150 GPa) [19,20]. Other attractive advantages of CNC are their low density (about 1.566 g cm^3), biocompatibility, and biodegradability [21]. Additionally, CNC can be extracted from abundant and renewable natural sources [22]. It has been widely demonstrated that the incorporation of CNC into biopolymers can result in bio-nanocomposite materials with a good appearance and high mechanical, thermal, and barrier properties [3,19,23-25], which are the main properties required for packaging applications [1,26].

The solvent casting method is frequently used for the processing of biopolymer blend and bio-nanocomposite films for food, pharmaceutical, and cosmetic packaging applications [27]. The interfacial adhesion and the condition of mixing during fabrication of biopolymer-based films, via the solvent casting method, strongly affect the network structure, physical properties, and film performance. Also, in the film casting process, the final film quality is strongly related to the rheological behavior of the film-forming solutions (FFS). Therefore, knowledge of the FFS rheological properties is important for the design and processing of films by casting [28-30]. The rheological properties of FFS based on biopolymer blends and

bio-nanocomposites can affect their spreadability during casting process and the thickness, uniformity and performances of resulting cast films [30]. Additionally, the formation of 3D-interconected network via strong interfacial interactions between nanofillers and macromolecular chains of polymers can be also deduced from the rheological properties [24]. The mechanical properties of CNC-reinforced biopolymer bio-nanocomposite cast films are often reported in the literature, but the FFS state and their rheological properties prior to the casting have received only limited attention.

Owing to their wide availability and good biodegradability as well as their good film-forming ability, films prepared from neat PVA or CMC have relatively poor mechanical and high water vapor permeability properties, which can limit their use as food packaging materials. Nevertheless, these drawbacks can be overcome by blending these biopolymers in a new PVA/CMC material, that can play the role of a new polymeric matrix for manufacturing bio-nanocomposites by using nanostructured fillers (such as CNC), without compromising the transparency and biodegradability of the original biopolymers. The aim of this work is to use the PVA/CMC blend as new biopolymeric matrix for developing bio-nanocomposite films, with improved water vapor permeability (WVP) and mechanical properties, using CNC isolated from sugarcane bagasse as nanoreinforcing agents. Previous experimental results showed that the composition 50/50 of CMC/PVA exhibits an enhanced properties [14-16]. This indicates the compatibility between PVA and CMC at this ratio. Such compatibility arises due to the presence of the carboxymethyl groups bonded to some of the hydroxyl groups on the cellulose in CMC and the hydroxyl groups in PVA capable of hydrogen bonding. In addition, the presence of hydroxyl groups on the surface of CNC ensures their compatibility with the PVA/CMC biopolymer blend. This compatibility between the CNC and the PVA/CMC blend can cause noncovalent interactions, therefore

driving the high reinforcement effect of CNC in resulting PVA/CMC–CNC bio-nanocompsoites. The rheological properties of FFS and the structural, transparency, thermal stability, tensile, and WVP properties of the resulting bio-nanocomposite films were evaluated and further discussed in this report. The results are very important for evaluating such films' possible applications as packaging material.

2. Materials and experimental details

2.1. Materials

Sugarcane bagasse fibers (SCB) was obtained from the SUNABEL-COSUMAR Group in Morocco. The moisture content of the raw SCB fibers was about 7 wt%. PVA (86–89 % hydrolyzed) and CMC were purchased from Alfa-Easer. Analytical grade chemicals used in this work were purchased from Sigma-Aldrich and used without further purification.

2.2 Isolation and characterization of Cellulose nanocrystals

The CNC aqueous suspension was prepared from SCB by using the sulfuric acid hydrolysis process, according to our previous work [31].

2.3. Bio-nanocomposite films processing

Bio-nanocomposite films were produced by the casting/evaporation technique. To begin, PVA solution was obtained by dissolving1.5 g of the PVA powder in 40 mL of water under stirring for 1 hour at 90 °C. Simultaneously, 1.5 g of CMC powder was dissolved in 150 mL of water under stirring for 2 hours at ambient temperature. After cooling down to room temperature, the both PVA and CMC solutions were mixed together under stirring for 1 hour at ambient temperature, resulting in a homogeneous solution of PVA/CMC (50/50 w/w). Thereafter, CNC aqueous suspension containing the desired amount of CNC (0.5, 2.5, 5, 10 wt%) was added to the PVA/CMC mixture under stirring for 30 min. Next, the obtained PVA/CMC-CNC film-forming solutions were sonicated for another 30 min.

Comment citer ce document :
Achaby, M. E., Miri, N. E., Aboulkas, A., Zahouily, M., Essaid, B., Barakat, A., Solhy, A. (2017). Processing and properties of eco-friendly bio-nanocomposite films filled with cellulose nanocrystals from sugarcane bagasse. International Journal of Biological Macromolecules, 96, 340–352. DOI : 10.1016/j.ijbiomac.2016.12.040

Subsequently, the PVA/CMC-CNC film-forming solutions were casted onto Petri dishes, and the water was evaporated at ambient temperature for 2 days. Finally, the obtained films were dried for 4 hours at 80 °C for complete removal of the water. The PVA/CMC (50/50 w/w) blend film was also prepared according to the procedure mentioned above without the addition of the CNC. The films were coded as PVA/CMC, PVA/CMC-CNC-0.5, PVA/CMC-CNC-2.5, PVA/CMC-CNC-5, and PVA/CMC-CNC-10. The number indicates the weight fraction of CNC.

2.4. Characterization techniques

Atomic force microscopy (AFM) was performed with a Veeco Dimension ICON. The tapping mode was used to capture height images at a scan rate of 1.5 Hz. The sample used for AFM characterizations was deposited from a CNC dispersion on a mica sheet. Transmission electron microscopy (TEM) for CNC characterization was performed using a Philips CM200 microscope operating at 80 kV. Droplets of CNC suspensions were deposited on glow-discharged carbon-coated grids. The liquid in excess was blotted away with filter paper and a drop of 2% (w/v) uranyl acetate negative stain was added prior to drying. Zeta potential and diameter distribution, via dynamic light scattering (DLS), of CNC aqueous suspension were carried out using a Malvern Zetasizer Nano ZS instrument. Measurements were made at 23 °C using 1 mL of diluted CNC suspension. Immediately before being analyzed, the suspension was sonicated for 5 min in an ultrasonic bath and then transferred to a folded capillary cell (DTS 1060, Malvern Instruments). X-ray diffraction (XRD) characterization was performed with a Bruker D8 Discover using Cu K_a radiation (λ=1.54184 nm) in the 2θ range of 2–60° while the voltage and current were held at 45 kV and 100 mA, respectively.

The rheological measurements of all FFS were performed at 20 °C using a Physica MCR500 rheometer equipped with concentric cylinder geometry (CC27). The temperature was regulated by a Paar Physica circulating bath and a controlled Peltier system (TEZ 150P-C). Morphology of SCB based fibers and bio-nanocomposite films was evaluated using scanning electron microscope (SEM) (FEI, Quanta 200-ESEM) operated at 20 kV. For bio-nanocomposite films, the samples were frozen in liquid nitrogen and cryo-fractured before being coated by a thin conductive carbon layer to help improve SEM observations. Fourier transform infrared spectroscopy (FTIR) was performed on an ABB Bomem FTLA 2000 spectrometer equipped with a Golden Gate single-reflection ATR accessory. The experiments were carried out in the range from 4000 to 400 cm^{-1} with a resolution of 4 cm^{-1} and an accumulation of 16 scans. The FTIR spectra were taken in the transmittance mode. Ultraviolet–visible (UV-vis) spectroscopy of the bio-nanocomposite films was carried out using a PerkinElmer LAMBDA 1050 spectrophotometer. The film samples were placed directly in the spectrophotometer test cell, and the air was used as reference. The optical transmittance of the films was measured in the wavelength range of 200–800 nm. Thermogravimetric analysis (TGA) and its derivative (DTG) were conducted under nitrogen with a 10 °C/min heating rate from 25 to 700 °C, using a TGA-Q500 (TA Instrument). Tensile tests were performed using an Instron 8821S tensiometer. The tensile specimens were cut in rectangular shapes with dimensions of 80 mm in length and 10 mm in width. The gauge length was fixed at 30 mm, and the speed of the moving clamp was 5 mm/min. All tests were performed on a minimum of five samples, and the reported results are average values. The determination of the WVP of the films was carried out according to the standard method E96-E95 (ASTM method 1995) with some modifications [6]. Glass bottles, with diameter of 20 mm and depth of 45 mm, were used to accomplish the test. About 4 g of

anhydrous $CaCl_2$ was placed inside each glass bottle, which was maintained at a relative humidity (RH) of 0%. The glass bottles were covered with the elaborated films, weighed, and inserted in a climatic chamber with RH of 50 % and temperature of 32 °C. The weighing was conducted each hour over a duration of 7 hours. The changes in the weight of the glass bottle were recorded as a function of time. Slopes were calculated by linear regression (weight change vs. time). The water vapor transmission rate (WVTR) was determined as the slope of the straight line (g/h) divided by the area of the glass bottle mouth (m^2). Finally, the WVP (g•m/m^2•h•Pa) was calculated as follows:

$$WVP = \frac{\mathrm{WVTR}}{\Delta\,\mathrm{p}} X = \frac{\mathrm{WVTR}}{S(\mathrm{R1} - \mathrm{R2})} X$$

where X is the thickness of the film (m), S is the saturation vapor pressure (Pa) at the test temperature (32 °C), and *R1* and *R2* are the relative humidity in the climatic chamber and the glass bottle, respectively.

3. Results and discussion

3.1 Characterization of SCB, treated SCB and CNC

The CNC used as nanoreinforcing agents have been extracted from SCB throughout the three well know steps, alkali and bleaching treatments, followed by acid hydrolysis process [31]. Figure 1a presents a photograph of the initial ground SCB showing a yellow-brown color. The SEM images (Figures 1b,c) shows that the raw SCB fibers exhibit a fibrous structure, and each fiber appeared to be composed of several fibrils. These fibrils were associated in small bundles and cemented by non-cellulosic compounds, showing a complete and compact structure along each elementary SCB fiber, and exhibiting an alignment in the fiber axis direction as shown Figure 1c. The alkali and bleaching treatments of raw SCB fibers resulted in bleached fibers with a clearly white color (Figure 1d).

Consequently, these white colored fibers might have contained pure cellulose, thus confirming that the noncellulosic elements, especially lignin and hemicelluloses, were totally removed under the alkali and bleaching treatments. Indeed, this bleaching treatment can result in the total defibrillation of raw fibers into individual microfibrils with smaller diameter (5-10 µm), as shown by SEM observations in Figures 1e,f. These microfibrils are very long which is characteristic of cellulose fibers that consist of both crystalline and amorphous domains. The yield of this bleached fibers was about 33 % in regard to the initial amount of raw SCB.

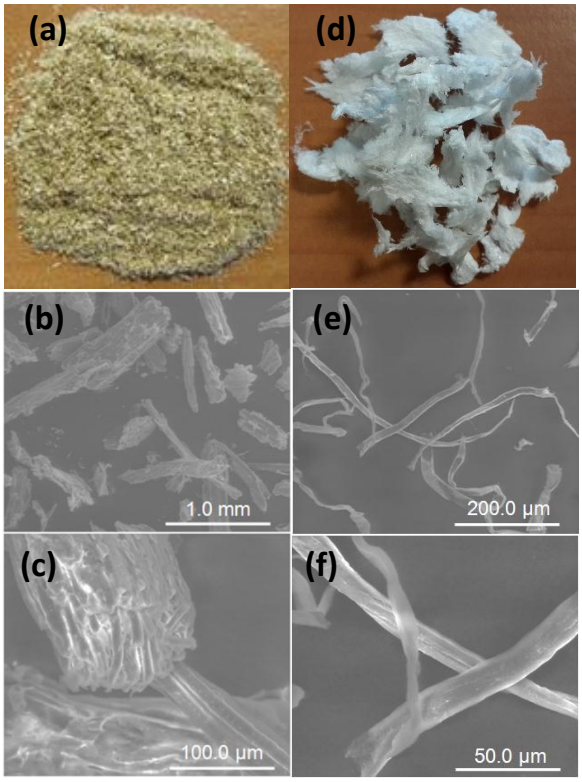

Figure 1: Digital photographs and SEM images of (a,b,c) raw SCB fibers and (d,e,f) bleached SCB fibers.

In order to obtain sulfuric acid hydrolyzed-CNC, the as-obtained bleached SCB fibers were subjected to acid hydrolysis treatment, which was performed under appropriate conditions that allowed the removal of amorphous domains from the bleached cellulose

fibers. The removal of amorphous domains, via acid hydrolysis, was performed by cleaving cellulose microfibrils into bundles of CNC with nanometric dimensions, becoming more or less individualized by homogenization process with the ability to be obtained in CNC aqueous suspension as a white gel (Figure 2a). It is well know that the sulfuric acid hydrolyzed CNC are stable in water, as visually observed in Figure 2a, , which is a crucial property in the preparation of nanocomposite materials. The good stability of the CNC aqueous suspension is caused by the exclusion of apolar components, the insertion of polar sulfate groups during acid hydrolysis, and the exposition of -OH groups from the cellulose structure [3]. Additionally, the stability behavior can be deduced from the zeta potential measurements. For the obtained CNC suspension, the zeta potential had a mean value of −39.6 mV. The suspension of CNC was considered stable because the absolute value was higher than 25 mV [31]. After their separation from water *via* freeze drying process, a white powder of CNC was obtained (Figure 2b). The CNC yield was 15 % and 45 % in regard to the initial dry mass of raw SCB fibers and bleached SCB fibers, respectively. Comparatively, this yield is similar to the CNC derived from corncob (46-50 %) [32], higher than that obtained from rice straw (13-18 %) [33], and smaller than that obtained for CNC extracted from pineapple leaf (55-77 %) [34] and SCB (50-58 %) [35].

The morphology and size of the as-obtained CNC were characterized by AFM and TEM analysis. Example of the obtained micrographs from AFM and TEM observations are shown in Figure 2c and Figure 2d, respectively. These micrographs show that the as-isolated CNC had needle-like nanoparticles, thus confirming that their extraction from the treated SCB was successful. Additionally, the AFM and TEM images showed that the as-obtained CNC are uniform in diameter and irregular in length. In general, the morphology and size of the CNC are strongly related to the nature of the original raw material and hydrolysis conditions

or pretreatments [36]. Herein, the average diameter of the as-extracted CNC is 5±1.1 nm, and the average length is 275±73 nm, resulting in an average aspect ratio of about 55. In terms of aspect ratio, the obtained results are in harmony with the results reported for CNC extracted from SCB (32–64) [35], corncob (52-63) [32], sisal (43–60) [37], and pineapple leaf (50-60) [34]. The particle size distribution in term of equivalent spherical hydrodynamic diameter from DLS resulted in two main groups: 81.7 % of the particles were around 212.3 nm, and 18.3 % were around 20.74 nm (Figure 2e). Because CNC are nonspherical in shape, the particle size measured by light scattering does not directly relate to the true particle dimensions, and it cannot be related precisely to the CNC's diameter and length dimensions measured from AFM or TEM.

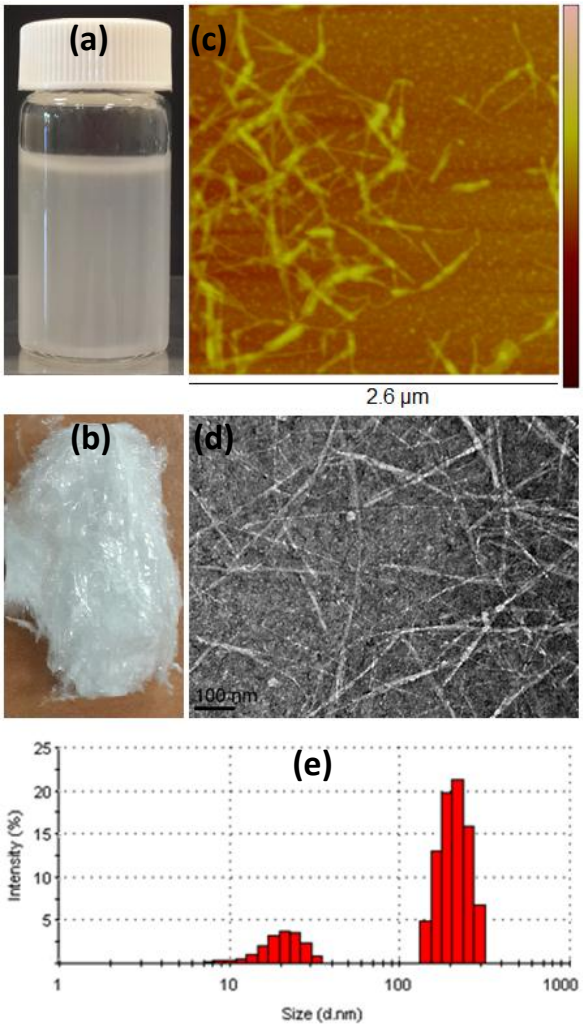

Figure 2: Photographs of (a) CNC aqueous suspension and (b) freeze-dried CNC, (c) AFM image of CNC, (d) TEM image of CNC and (e) particle size distribution of CNC from DLS measurement.

The crystalline structure and the crystallinity index of raw SCB fibers, bleached SCB fibers and nanosized CNC were determined using XRD analysis. The XRD patterns (Figure 3a) show that the major peaks are located at 2θ values of around 14.9°, 16.3°, 22.6° and 34.5°, which correspond to the (110), (11$\bar{0}$), (002), and (004) planes. These results indicate that there is a predominance of crystalline structure of cellulose I for all cellulosic samples [35, 38]. Though the XRD data of raw SCB and bleached SCB fibers display a small amount of cellulose II polymorph, which can be verified by the presence of small peak

observed at 2θ=11.7° and 20.5°. Contrary, the hydrolyzed CNC exhibit only a crystalline structure of cellulose I. From the XRD data, the crystallinity index (*CrI*) of raw SCB, bleached SCB and CNC was found to be 19 %, 45 % and 78 %, as determined from the equation $CrI = ((I_{002} - I_{amorph})/I_{002}) \times 100$, where I_{002} and I_{amorph} are the peak intensities of crystalline and amorphous cellulose, respectively [35,38].

The thermal degradation of all cellulosic samples (raw SCB, treated SCB and CNC) was investigated using thermogravimetric analysis, and the obtained TGA/DTG curves are illustrated in Figure 3b. Remarkably, the onset temperatures (T_{onset}) of raw SCB, treated SCB and CNC were observed at 239, 279 and 153 °C, and the corresponding maximum temperatures (*Tm*) were observed at 355, 359 and 230 °C, respectively. The lower T_{onset} and T_m observed for CNC, as compared to those of raw SCB and bleached SCB, is due to the insertion of sulfate groups in the surface of CNC during hydrolysis with sulfuric acid.

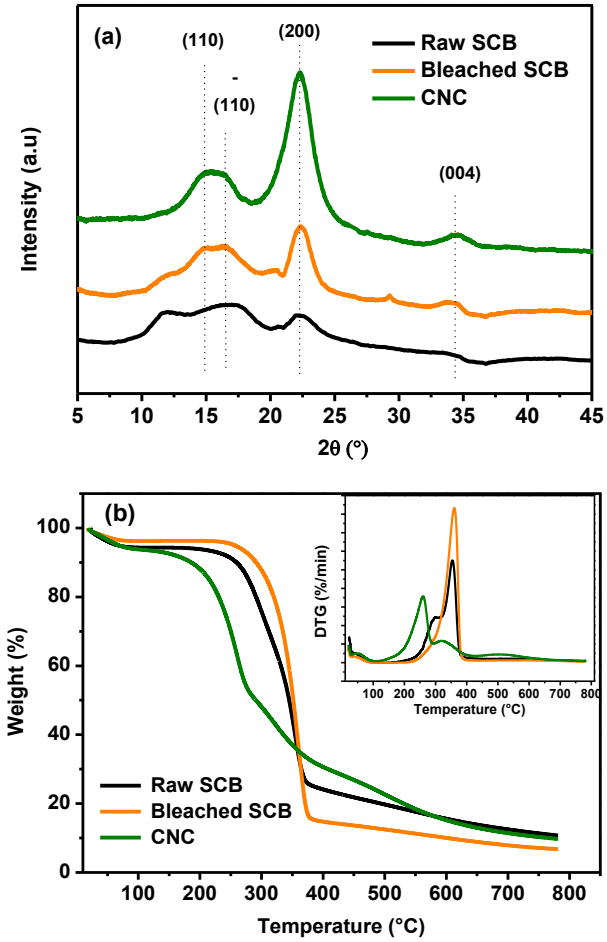

Figure 3: (a) XRD patterns and (b) ATG/DTG curves of raw SCB fibers, bleached SCB fibers and CNC.

3.2 Processing of films

It is well known that the PVA and CMC are miscible and compatible polymers via hydrogen bonding interactions. Such behavior is due to the presence of the carboxyl and hydroxyl groups in CMC and the hydroxyl groups in PVA, which can result in the formation of hydrogen bonds [13-16], as illustrated in Figure 4. Also, their mixture in water can easily be achieved due to their hydrophilic nature. Interestingly, the hydrolyzed CNC exhibit free hydroxyl groups on their surfaces, which can also strongly interact with the free

hydroxyl groups of the PVA and the free hydroxyl and carboxyl groups of the CMC. When CNC are added to the PVA/CMC blend mixture, an interconnected bond network can form through strong interactions, as schematically proposed in Figure 4. This large compatibility between the three components (PVA, CMC and CNC) enabled the formation of homogeneous and stable FFS when they were mixed in controlled conditions. By casting the resulted FFS on plastic dishes and evaporating the water, 70-µm-thick films were produced with high quality, smooth surface, and good flexibility.

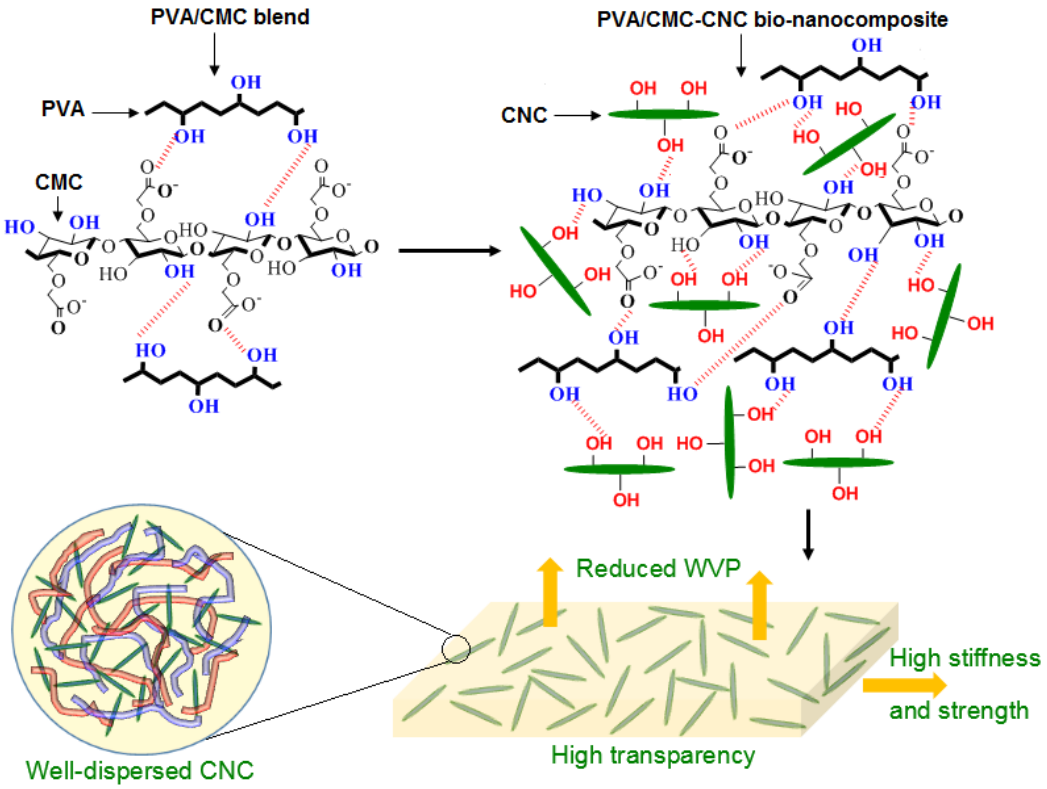

Figure 4: Schematic representation of intermolecular hydrogen bonds that occurred in PVA/CMC blend and PVA/CMC-CNC bio-nanocomposites and the structure of the resulting bio-nanocomposite films with well-dispersed CNC.

3.3 Rheological behavior of film-forming solutions

The rheological properties of FFS are important for the design and processing of films by casting [28,29]. To make a film with high quality, the viscosity of FFS should be such that it can prevent sagging by gravity and allow capillary leveling [29,39]. Furthermore, Cuq et al. reported that it is very difficult to eliminate air bubbles from biopolymers-based FFS with high-viscosity and the casting process cannot be achieved [40]. According to this, a mixing equipment is necessaire to cast a high quality film from high-viscosity FFS. Nevertheless, the FFS must be characterized by a relatively low viscosity to avoid retention of air bubbles and to cast thin films with high quality [29].

In this work, before the casting of films, the rheological behavior of FFSs was investigated to evaluate the effect of the addition of CNC on the viscosity and the viscoelastic behavior of the PVA/CMC polymeric blend. Figure 5a shows the results of the steady shear viscosity (η) for the all studied FFS. From this figure, the PVA/CMC FFS exhibited Newtonian behavior at low shear rates (< 10 s^{-1}) and shear-thinning behavior at high shear rates (> 10 s^{-1}), which can be explained by the breakage of interacted macromolecular chains during the rotational measurements [41]. The shearing results also indicate that the PVA/CMC FFS behaves as an entanglement network system (or a concentrated solution) [42,43]. The same behavior was observed for PVA/CMC-CNC-0.5 FFS with a slight increase in the shear viscosity at low shear rate, which may be due to the formation of hydrogen bonding between the macromolecular chains of the PVA/CMC and the functional groups of the CNC.

The FFS of the PVA/CMC-CNC bio-nanocomposites containing more than 0.5 wt% CNC (i.e., 2.5, 5, and 10 wt%) showed only shear thinning behavior in the full shear rate range.

This finding indicates that the CNC are well dispersed and forms an interconnected network structure within bio-nanocomposites mixtures throughout hydrogen interactions, causing the increase of the viscosity [44]. A similar trend was reported for CNC-filled poly(ethylene oxide) film-forming solutions, in which the incorporation of CNC causes the transition from Newtonian behavior to shear thinning behavior in the full range of shear rate [44], which was related to the construction of a network structure of CNC throughout interfacial interactions [44,45].

With regard to the casting process and film appearance, the prepared FFS were highly stable, forming homogeneous mixtures without air bubbles, and no phase separation was observed in all FFS. In consequence, the shear viscosity obtained for all FFS was appropriate for films casting since uniform layers of FFS were spread on the Petri dishes, covering the entire surface at room temperature. As a result, the dried films were smooth, homogeneous, and transparent, and were easily peeled off from the plate surface. Additionally, these films were optically transparent, as confirmed by UV–Vis transmittance measurements and visual observations.

Dynamic frequency sweep tests were performed in the linear viscoelastic range to determine the frequency dependence of the storage modulus (G') and loss modulus (G"). It should be noted that the dynamic frequency sweep results can be used to characterize or classify polymer-based solutions [46]. According to the results of G' and G", the four most traditional classifications are a dilute solution, an entanglement network system, a weak gel, and a strong gel [46]. As shown in Figure 5b, the G' and G" values increased as the frequency increased for all FFSs. Furthermore, these values increased as the content of CNC increased for the bio-nanocomposite FFSs, suggesting that the CNC were well dispersed at the nanoscale within the PVA/CMC blend solution. Since G' usually describes the elastic

behavior and G" represents the viscous behavior, enhancement in structural entanglement increases the G' modulus, while structural breakdown increases the G" modulus [28,41]. Accordingly, the data in Figure 5b indicate that all FFSs show predominantly viscous behavior (liquid-like) at low frequencies (G'<G'') and elastic behavior (solid-like) at high frequencies (G'>G''). This type of behavior is indicative of an entanglement network system, which is characterized by the intersecting of both moduli (G''= G') at the middle of the frequency range (cross-over point), indicating a clear tendency for solid-like behavior at higher frequencies [30,41,46]. These results strongly align with those previously reported in the literature [30,39,42,43]. Furthermore, Peressini et al. reported that the elastic behavior is a function of the number of effective chains participating in the formation of an entangled network structure [39]. The increase in G' values with the addition of CNC to the PVA/CMC solution suggested the presence of a greater number of interacting chains than that for the PVA/CMC solution. In the FFS of the PVA/CMC blend, the entangled network was caused by inter-chain interactions between the macromolecular chains of PVA and CMC. However, in the FFS of the PVA/CMC-CNC bio-nanocomposite, the dispersion of CNC can cause additional interfacial interactions between their functionalized surfaces and the macromolecular chains of PVA and CMC (Figure 4).

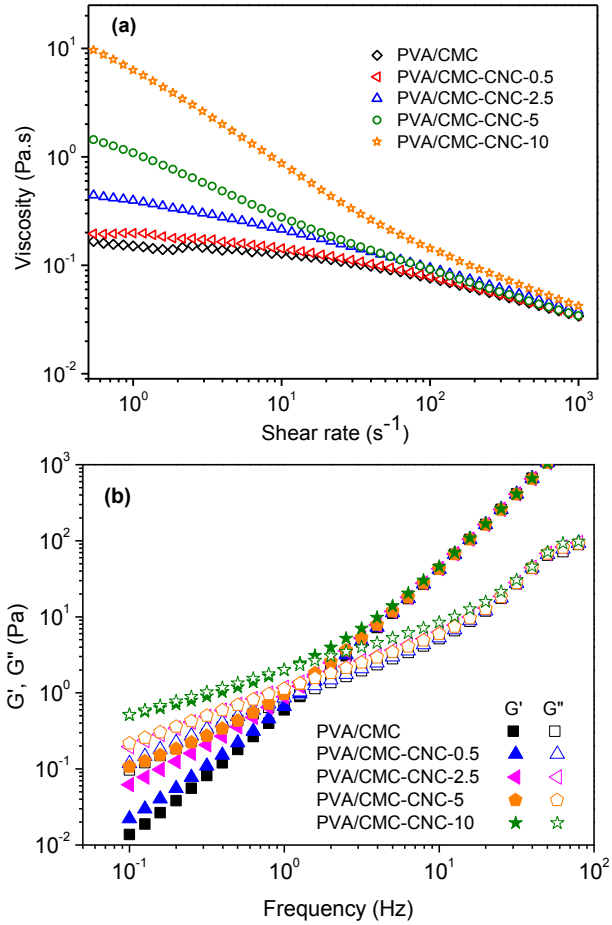

Figure 5: (a) Shear viscosity versus shear rate and (b) storage modulus and loss modulus versus frequency of FFS of PVA/CMC blend and PVA/CMC-CNC bio-nanocomposites.

3.4 SEM analysis of bio-nanocomposite films

Figure 6 presents SEM photographs of the cryo-fractured sections of films. Figure 6a shows that the cross-section of the PVA/CMC film without CNC is smooth without any cracks and pores. For bio-nanocomposite films (Figures 6b-d), it was observed that the cross-section is relatively rougher than that observed for PVA/CMC film without CNC. In bio-nanocomposites containing up to 5 wt% CNC, no obvious aggregations of CNC and microphase separation were observed in the SEM photographs (Figures 6b-c). This finding indicates that CNC were dispersed homogenously within the PVA/CMC blend. In contrast, a slight agglomeration of CNC can be clearly observed in the bio-nanocomposite containing

10 wt% CNC (Figure 6d). This effect is mainly due to the existence of strong interactions between the surface hydroxyl groups of the CNC at the higher loading level; consequently, the nanocrystal–nanocrystal interaction becomes dominant over the nanocrystal–matrix interaction [25,47].

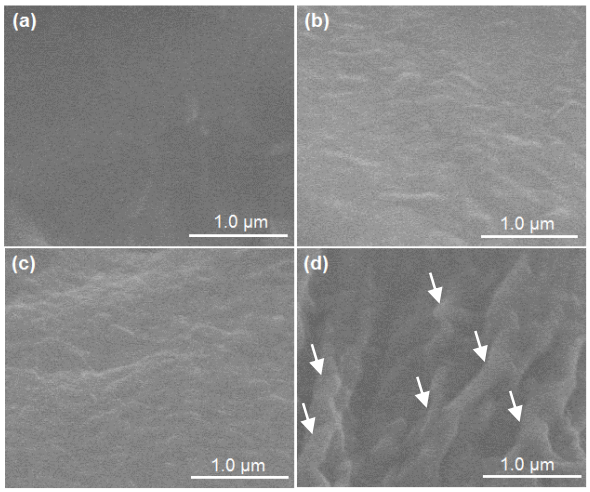

Figure 6: SEM micrographs of (a) PVA/CMC, (a) PVA/CMC-CNC-2.5, (b) PVA/CMC-CNC-5 and (c) PVA/CMC-CNC-10 films.

3.5 FTIR analysis of bio-nanocomposite films

Figure 7 shows the FTIR spectra of PVA, CMC, PVA/CMC blend, freeze dried CNC and PVA/CMC-CNC-5 bio-nanocomposite. For neat PVA, the bands at 3290 and 1478 cm^{-1} are assigned to -OH stretching and bending vibrations hydroxyl group (-OH). The band corresponding to methylene group (CH2) asymmetric stretching vibration occurs at about 2987 cm^{-1}. The vibrational band at about 1743– 1586 cm^{-1} corresponds to C=C stretching of PVA. The band at approximately 1124 cm^{-1} corresponds to C-O stretching, and that at about 1780 cm-1 to C=O stretching of the unhydrolyzed ester functional group present on the PVA backbone. For neat CMC film spectrum, the band at 1055 cm^{-1} can be associated to C-O stretching vibration of ether groups, while the bands at 1434 and 1604 cm^{-1} is attributed to the asymmetric and symmetric modes of stretching vibration of carboxylate groups

(C=O), respectively, and the broad band centered at 3338 cm−1 is attributed to the stretching of OH groups and intermolecular and intramolecular hydrogen bonds.

The PVA/CMC blend and PVA/CMC-CNC bio-nanocomposite spectra exhibited in general the same peaks as those found in the neat PVA and CMC due to the equal amount of each polymer in the blend, as shown in Figure 7. Owing to the chemical similarities between CMC and CNC (except for carboxylate groups in CMC) and the relatively low content of CNC (5.0 wt%) within the PVA/CMC-CNC bio-nanaocomposite films, all peaks of CNC were overlapped with those of CMC. Importantly, the intensity of absorption bands of C=O (1780 cm^{-1}) and C-O (1055 cm^{-1}) of CMC were significantly decreased, and the broad bands of hydroxyl groups of each polymer were overlapped in a new peak centered at 3307 in PVA/CMC blend, suggesting the presence of interactions between the hydroxyl and carboxylate groups of CMC and the hydroxyl groups of PVA and CN. These findings have been also reported for PVA/CMC blend [14], CNC-filled CMC/Starch blend [3], CNC-filled PVA [22], and graphene oxide-filled PVA [48] nanocomposite films.

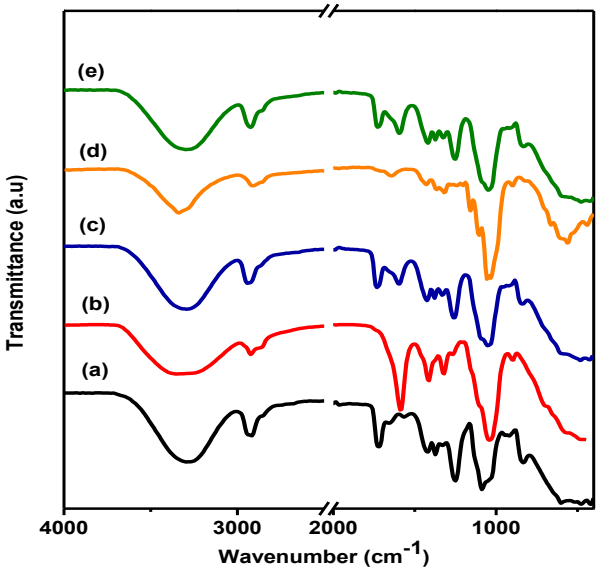

Figure 7: FTIR spectra of (a) PVA, (b) CMC, (c) PVA/CMC, (d) freeze-dried CNC and (e) PVA/CMC-CNC-5 bio-nanocomposite films.

3.6 Transparency properties of films

Transparency is a desirable feature of films for food packaging; a transparent film allows the packed product to be seen [17,49]. It is well known that PVA and CMC are transparent polymers, with the transparency level being higher than 90 % in the visible light region [3,13]. As seen in the Figure 8, the PVA/CMC blend film also has a high transparency level (≈ 90 %) in the wavelength range of 400-800 nm, indicating that the film prepared from blending PVA and CMC was homogeneous and had a high quality, which is due to the good compatibility and miscibility between the PVA and CMC polymers [14]. Importantly, when CNC were added to the PVA/CMC polymer blend, all PVA/CMC-CNC bio-nanocomposite films maintained the same transparency as the PVA/CMC blend matrix (≈90 %), confirming that the CNC were well dispersed in the bio-nanocomposite films [22,23]. It also confirmed that CNC have good compatibility with the PVA/CMC polymeric blends. This condition avoids CNC aggregation and thus reduces the amount of light scattering, favoring the transmittance of visible light through the bio-nanocomposite films [3]. This is directly related to the strong interfacial interactions between the macromolecular chains of polymers and the surface of the CNC.

The photographs of films are presented in the bottom of Figure 8, showing that the transparency of the PVA/CMC blend film was not affected by the incorporation of CNC due to its good dispersion within bio-nanocomposite films [22,23]. In conclusion, the results from the transmittance UV–Vis measurements and the visual observations of the films confirm the efficiency of the processing procedure of bio-nanocomposite films, which could be used as active materials in food packaging applications.

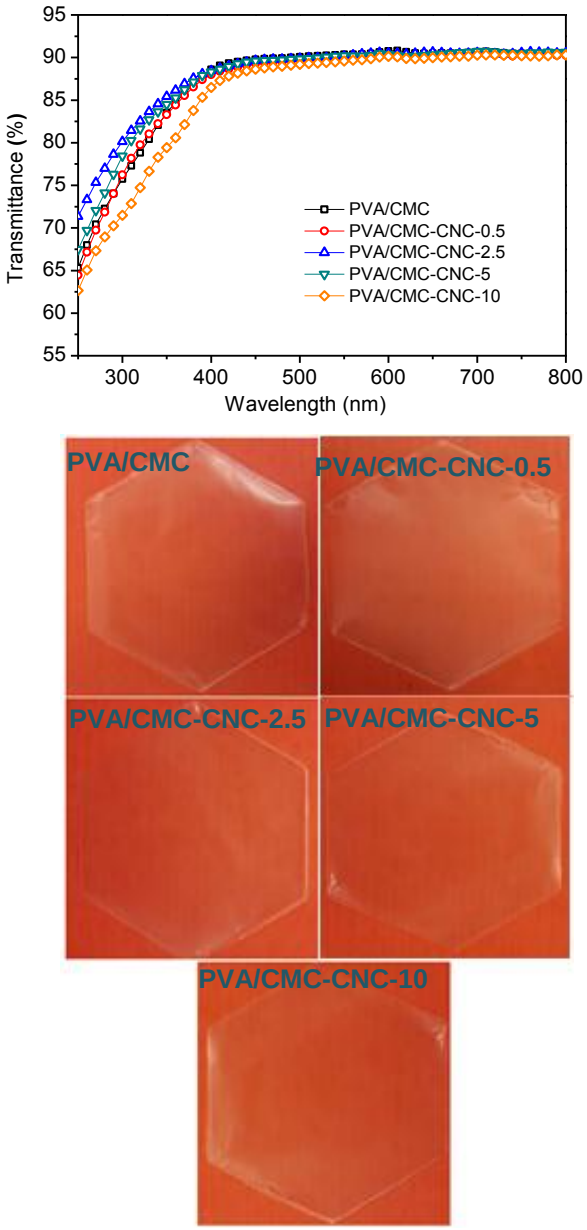

Figure 8: UV-Vis transmittance (top) and digitals images (below) of PVA/CMC blend and PVA/CMC-CNC bio-nanocomposite films.

3.7 WVP of bio-nanocomposite films

The WVP was analyzed for the addition of CNC to PVA/CMC film. The WVP is a highly important property to consider in food packaging materials. Because the film should avoid or at least decrease moisture transfer between food and surrounding atmosphere; the WVP should be as low as possible [3,49]. Figure 9 compares the WVP of PVA/CMC blend

film and its bio-nanocomposites with CNC. It is interesting to note that the PVA/CMC blend film without CNC exhibited a much greater WVP value (1.16×10^{-7} g•m/Pa•h•m^2). It is well known that the PVA and CMC polymers are highly sensitive to moisture and exhibit poor water vapor barrier properties due to their hydrophilic character, which enormously restricts their application in the packaging industry [17,18]. Surprisingly, the addition of CNC into the PVA/CMC blend had a positive effect on the WVP of the resulting PVA/CMC-CNC bio-nanocomposite films. The WVP of bio-nanocomposite films decreased to 1.07×10^{-7}, 0.72×10^{-7}, 0.21×10^{-7}, and 0.22×10^{-7} g•m/Pa•h•m^2 when 0.5, 2.5, 5, and 10 wt% CNC were added, respectively. These results might be attributed to the network formed by the homogeneous dispersion of CNC within the polymeric blend and hydrogen bonds between the oxygen-containing groups of PVA/CMC and the functional groups of the CNC (Figure 4). This network and the hydrogen bonds reduced the free volumes of the bio-nanocomposite films and increased the tortuosity of the water molecule pathway through these films [3,47,50], thus reducing the WVP of the PVA/CMC-CNC bio-nanocomposite films (Figure 9). Remarkably, at 10 wt % CNC, the WVP increased slightly compared to the 5 wt % CNC bio-nanocomposite. This difference is because CNC tend to agglomerate within the polymeric blend as the filler–filler interaction becomes dominant over the filler–matrix interaction, inevitably facilitating the diffusion of water vapor. The same WVP-related behavior of CNC has been reported with other biopolymer-based nanocomposite films, such as PVA/CNC [50] and CMC/cotton linter cellulose nanofibril [47].

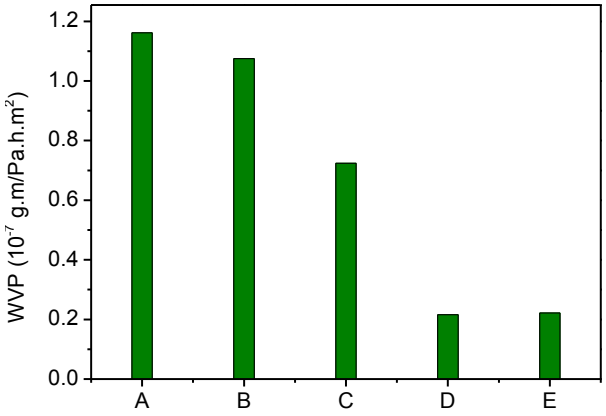

Figure 9: WVP of (A) PVA/CMC blend and (B,C,D,E) PVA/CMC-CNC bio-nanocomposite films at CNC content of 0.5, 2.5, 5 and 10 wt%, respectively.

3.8 Thermal stability of films

The TGA and DTG are considered the best methods for studying the thermal stability of polymers and polymer based nanocomposites. Herein, the thermal stability of the PVA/CMC matrix blend and PVA/CMC–CNC bio-nanocomposite films was studied in a nitrogen atmosphere. From TGA/DTG curves (Figure10), the PVA/CMC blend and its bio-nnaocomposites shown a three steps-decomposition pattern. The first weight loss observed at about 100 °C was related to the evaporation of absorbed water. In addition, the weight loss at around 300 °C could be related to the polymer dehydration process, and the third weight loss observed at around 430 °C is due to the decomposition of polymer main chains [51]. From TGA/DTG curves, the onset temperature (T_{onset}), the temperature corresponding to a weight loss of 20 % ($T_{20\%}$), the maximum temperature (T_{max}) and the residual weight (*RW*) were obtained and summarized in the Table 1. Furthermore, T_{onset} of PVA/CMC control was not largely affected by the addition of CNC, except for the bio-nanocomposite containing 10 wt% CNC, which had a lower T_{onset} (Table 1). This may be due to the agglomeration phenomenon of CNC within the polymer matrix. Unfortunately, the CNC are thermally unstable nanomaterials, and the degradation process starts at 153 °C (Figure 3b),

because of the presence of sulfate groups on their surface [3]. Subsequently, after the incorporation of the CNC into the polymer matrix, the major mass loss (≈50 %) occurring between 153 and 300 °C disappeared, suggesting a good interaction between the functional groups of CNC and the macromolecular chains of PVA/CMC polymer blend. This was confirmed by increasing of the $T_{20\%}$ and T_{max}, in which these temperatures for the bio-nanocomposites are higher than those observed for PVA/CMC without CNC (Table 1). The measured values of residual weight (*RW*) at 500 °C showed that incorporation of CNC into PVA/CMC blend has slightly influenced the measurement. The residual weight was observed in the range 31-34 %, except for bio-nanocompsoite containing 5 wt% CNC, in which a lower RW was observed (~ 24 %). These variations in *RW* could be related to the interfacial interactions between components and the presence of sulfate groups on the surface of CNC, which can be acted as dehydration catalyst and facilitates the char residue formation [52].

Table 1: Onset temperature (T_{onset}), temperature corresponding to a weight loss of 20 % ($T_{20\%}$), maximum temperature (T_{max}) and residual weight (RW) obtained from TGA/DTG analysis.

	T_{onset} (°C)	$T_{20\%}$ (°C)	T_{max} (°C)	*RW* (%) at 500 °C
PVA/CMC	255	280	288	33.46
PVA/CMC-0.5	257	284	299	33.02
PVA/CMC-2.5	255	286	296	31.43
PVA/CMC-5	240	280	296	23.84
PVA/CMC-10	248	287	296	34.06

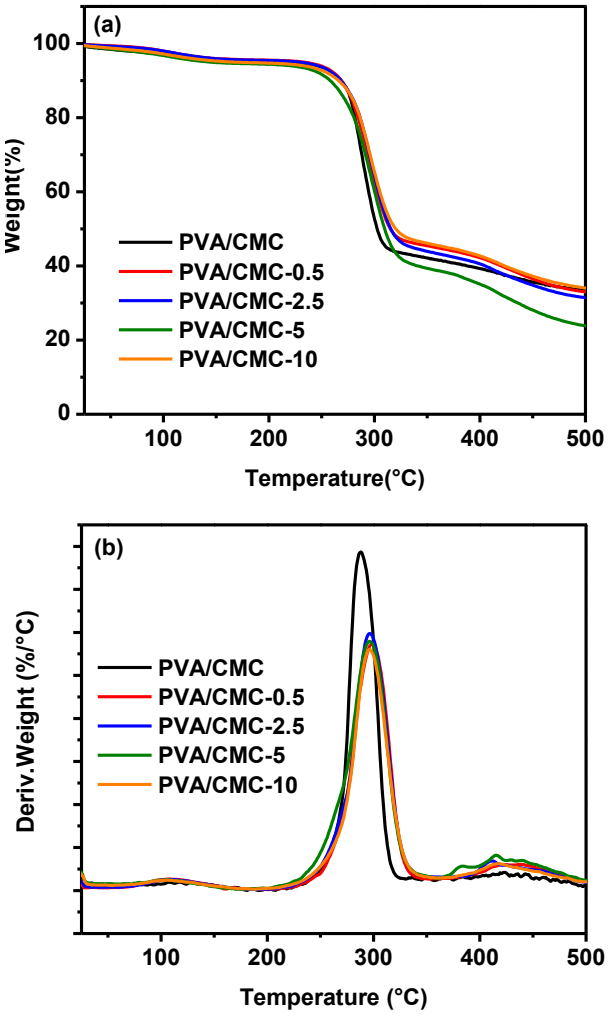

Figure 10: (a) TGA and (b) DTG curves of PVA/CMC blend, and PVA/CMC-CNC bio-nanocomposite films.

3.9 Tensile properties of films

The mechanical behavior of PVA/CMC based bio-nanocomposites was characterized by tensile tests. Typical stress-strain curves of all the studied bio-nanocomposite films are presented in Figure 11a. The tensile modulus, tensile strength, elongation at break and toughness were extracted from the stress-strain curves and plotted in Figures 11b and 11c as a function of CNC content; and the values of these selected properties are summarized in Table 2.

It is worth noting that the as-prepared PVA/CMC blend film without CNC presented a ductile behavior and displayed a relatively low elastic modulus and tensile strength that limits its use for application as a packaging material, in which a high stiffness and strength are required [53]. After the addition the CNC up to 5 wt%, the resulting PVA/CMC-CNC bio-nanocomposites clearly exhibited an increase in tensile modulus and tensile strength and a reduced elongation at break, which are typical results for the reinforcement of a polymer matrix. This could result from the high aspect ratio of the CNC. From our previous work [31], the neat PVA film exhibits a tensile modulus of 865.78 MPa, an ultimate tensile strength of 49.80 MPa, an elongation at break of 64.98% and , and a toughness of 23.44×10^8 J/m^3. From Figures 11b,c and Table 2, these selected tensile properties of the neat PVA were affected after blending in PVA/CMC film. It was observed that the novel blend film of PVA/CMC showed a tensile modulus of 1138.7 MPa, an ultimate tensile strength of 64.85 MPa, an elongation at break of 21.27 % and , and a toughness of 9.91×10^8 J/m^3. This trend was also observed for PVA/chitosan [54] blend. These variations in the tensile properties of PVA after its blending with CMC could be attributed to the establishment of bonds between the chains of both PVA and CMC polymers [55], as schematically presented in Figure 4, which reinforce the network structure, thus improving the mechanical strength of the films [55-57].

When 5 wt% CNC was added to PVA/CMC blend matrix, the tensile modulus and tensile strength were improved by 141 % and 83 %, respectively, meanwhile the toughness and elongation at break were decreased by 14 % and 55 %, respectively. In contrast, from our previous work [31], the tensile modulus and tensile strength of the PVA-based nanocomposite film containing 5 wt% CNC were increased only by 77 and 12%, respectively, as compared to neat PVA. Herein, in ternary PVA/CMC-CNC bio-

nanocomposite, the enhancement of tensile modulus and tensile strength could be attributed to the compact structure of PVA/CMC polymeric blend, and the presence of CNC as nanoreinforcing agents can restraint of the macromolecular chain movement of polymers during the deformation process, thus improving the tensile modulus and strength of the resulted bio-nanocomposite films. This behavior is induced by the formation of a bonded network that was generated by the addition of CNC within the PVA/CMC blend. This network was formed throughout the strong interactions and hydrogen bonding that occurred between the CNC and PVA/CMC polymer blend, as schematically illustrated in Figure 4. This trend was also observed by Almasi et al., when nanoclay particles were incorporated into CMC/starch polymeric blend [58]. Such improvements confirmed that the PVA/CMC-CNC bio-nanocomposite films have a high stiffness and strength, which are the main mechanical properties required for packaging applications.

However, once the CNC content exceeds 10 wt%, the tensile modulus remained almost constant, and the tensile strength started to decrease in the bio-nanocomposite containing 10 wt% CNC (Figure 11b). Additionally, the toughness and elongation at break were drastically decreased when 10 wt% CNC was added to PVA/CMC blend (Figure 11c). These results for high CNC content (10 wt%) are related to the agglomeration phenomenon of CNC within the PVA/CMC polymeric blend matrix, leading to a less pronounced increase in tensile modulus and strength [59,60].

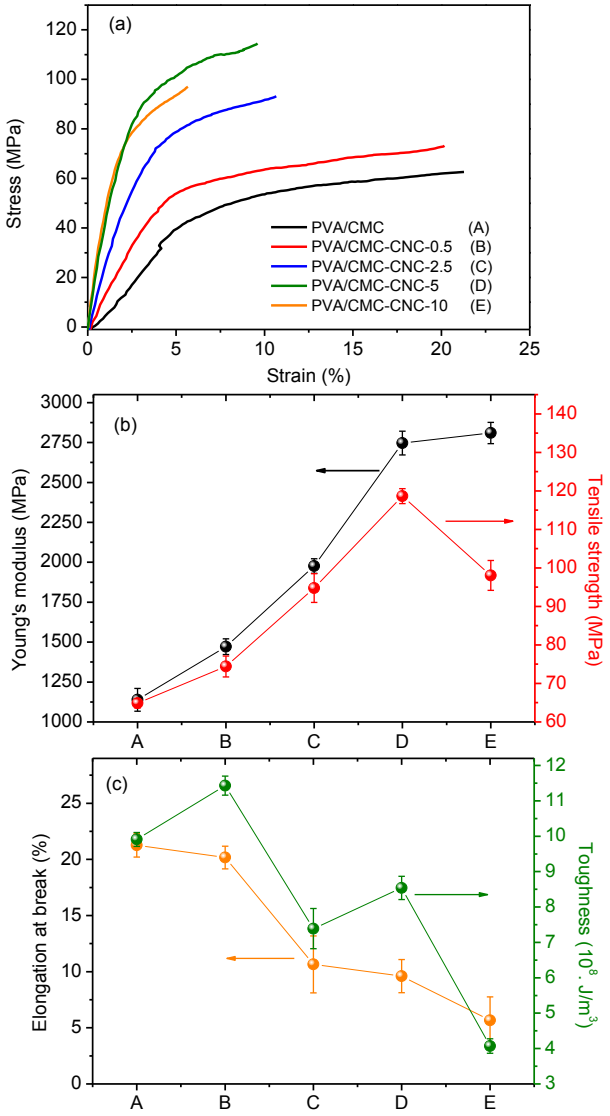

Figure 11: (a) Typical stress-strain curves, (b) tensile modulus and tensile strength, and (c) elongation at break and toughness of PVA/CMC blend and PVA/CMC-CNC bio-nanocomposite films.

Table 2: Tensile modulus (E), tensile strength (σ_s), elongation at break (ε_b) and Toughness (T) of PVA/CMC blend and PVA/CMC-CNC bio-nanocomposite films.

	E (MPa)	σ_s (MPa)	ε_b (%)	T (10^8 J/m^3)
PVA/CMC	1138.7±70.93	64.85±1.24	21.27±1.06	9.91±0.19
PVA/CMC-0.5	1471.46±49.57	74.41±2.72	20.17±1.11	11.43±0.27
PVA/CMC-2.5	1976.04±45.80	94.76±3.73	10.65±2.53	7.39±0.56
PVA/CMC-5	2746.9±74.34	118.65±1.93	9.6±1.48	8.54±0.32
PVA/CMC-10	2809.73±66.48	98.05±3.90	5.67±2.08	4.07±0.20

4. Conclusion

New eco-friendly bio-nanocomposite films based on cellulose nanocrystals (CNC) filled polyvinyl alcohol (PVA)/carboxymethyl cellulose (CMC) biopolymer blend were prepared *via* solvent casting films, and their properties were evaluated and discussed in this report. Due to the relatively high aspect ratio of CNC, extracted from sugarcane bagasse fibers, their incorporation into PVA/CMC blend shown a positive effect on the properties of the resulted bio-nanocompsoites films. Compared to PVA/CM control, CNC-based PVA/CMC bio-nanocomposites exhibited enhanced tensile modulus and tensile strength, and a reduced water vapor permeability. More importantly, bio-nancomposite films maintained the same transparency level of the PVA/CMC blend film, confirming that the CNC were dispersed in nanometric scale. The enhancement of the properties of the bio-nanocomposite films was due to strong interfacial interactions generated from the hydrogen bonding between the hydroxyl groups in the CNC and the hydroxyl and carboxyl groups in the PVA and CMC polymers. Consequently, these eco-friendly structured bio-nanocomposite films with superior properties are expected to be useful in food packaging applications.

Acknowledgments

The financial assistance of the Office Chérifien des Phosphates (OCP Group) in the Moroccan Kingdom toward this research is acknowledged. The authors would like to acknowledge SUNABEL-COSUMAR Company in Morocco for providing us the raw sugarcane bagasse. This work was performed as part of a collaboration between the Mohammed VI Polytechnic University and INRA-Montpellier. Financial support of the INRA-Montpellier is acknowledged.

References

[1] J.W. Rhim, H.M. Park, C.S. Ha, Bio-nanocomposites for food packaging applications, Prog. Polym. Sci. 38 (2013) 1629–1652

[2] Y. Kasirga, A. Oral, C. Caner, Preparation and characterization of chitosan/montmorillonite-K10 nanocomposites films for food packaging applications, Polym. Compos. 33 (2012) 1874–1882

[3] N. El Miri, K. Abdelouahdi, A. Barakat, M. Zahouily, A. Fihri, A. Solhy, M. El Achaby, Bio-nanocomposite films reinforced with cellulose nanocrystals: Rheology of film-forming solutions, transparency, water vapor barrier and tensile properties of films, Carbohydr. Polym. 129 (2015) 156–167

[4] Z. Rezvani, M. Shahbaei, Bionanocomposites based on alginate and chitosan/layered double hydroxide with ciprofloxacin drug: Investigation of structure and controlled release properties, Polym. Compos. 36 (2015) 1819–1825

[5] A. Sionkowska, Current research on the blends of natural and synthetic polymers as new biomaterials: Review, Prog. Polym. Sci. 36 (2011) 1254–1276

[6] B. Ghanbarzadeh, H. Almasi, A.A. Entezami, Physical properties of edible modified starch/carboxymethyl cellulose films, Innov. Food. Sci. Emerg. Technol. 11 (2010) 697–702

[7] N. Hameed, R. Xiong, N.V. Salim, Q. Guo, Fabrication and characterization of transparent and biodegradable cellulose/poly (vinyl alcohol) blend films using an ionic liquid, Cellulose 20 (2013) 2517–2527

[8] S. Salmieri, F. Islam, R.A. Khan, F.M. Hossain, H.M.M. Ibrahim, C. Miao, W.Y. Hamad, M. Lacroix, Antimicrobial nanocomposite films made of poly(lactic acid)-

cellulose nanocrystals (PLA-CNC) in food applications: part A—effect of nisin release on the inactivation of Listeria monocytogenes in ham, Cellulose 21 (2014) 1837–1850

[9] A.M. Youssef, S.M. El-Sayed, H.H. Salama, H.S. El-Sayed, A. Dufresne, Evaluation of bionanocomposites as packaging material on properties of soft white cheese during storage period, Carbohyd. Polym. 132 (2015) 274–285

[10] M. El Achaby, Y. Essamlali, N. El Miri, A. Snik, K. Abdelouahdi, A. Fihri, M. Zahouily, A. Solhy, Graphene oxide reinforced chitosan/polyvinylpyrrolidone polymer bio-nanocomposites, J. Appl. Polym. Sci. 131 (2014) 41042

[11] F. Rafieian, J. Simonsen, The effect of carboxylated nanocrystalline cellulose on the mechanical, thermal and barrier properties of cysteine cross-linked gliadin nanocomposite, Cellulose 22 (2015) 1175–1188

[12] S.K. Swain, S.K. Patra, S.K. Kisku, Study of thermal, oxygen-barrier, fire-retardant and biodegradable properties of starch bionanocomposites, Polym. Compos. 35 (2014) 1238–1243

[13] B. Gupta, R. Agarwal, M.S. Alam, Preparation and characterization of polyvinyl alcohol-polyethylene oxide-carboxymethyl cellulose blend membranes, J. Appl. Polym. Sci. 127 (2012) 1301–1308

[14] M.F. Abou Taleb, H.L. Abd El-Mohdy, H.A. Abd El-Rehim, Radiation preparation of PVA/CMC copolymers and their application in removal of dyes, J. Hazard. Mater. 168 (2009) 68–75

[15] S. El-Sayed, K.H. Mahmoud, A.A. Fatah, A. Hassen, DSC, TGA and dielectric properties of carboxymethyl cellulose/polyvinyl alcohol blends, Physica B 406 (2011) 4068–4076

[16] A.M. El Sayed, Synthesis and controlling the optical and dielectric properties of CMC/PVA blend via C-rays irradiation, Nucl. Instrum. Methods. Phys. Res. B 321 (2014) 41–48.

[17] S. Villarruel, L. Giannuzzi, S. Riveroa, A. Pinotti, Changes induced by UV radiation in the presence of sodium benzoate in films formulated with polyvinyl alcohol and carboxymethyl cellulose, Mater. Sci. Eng. C 56 (2015) 545–554

[18] S.R Muppalla, S.R Kanatt, S.P. Chawla, A. Sharma, Carboxymethyl cellulose–polyvinyl alcohol films with clove oil for active packaging of ground chicken meat, Food Packaging and Shelf Life 2 (2014) 51–58

[19] M.A.S. Azizi-Samir, F. Alloin, J.Y. Sanchez, A. Dufresne, Cellulose nanocrystals reinforced poly(oxyethylene), Polymer 45 (2004) 4149–4157

[20] A. Sturcova, G.R. Davies, S.J. Eichhorn, Elastic modulus and stress-transfer properties of tunicate cellulose whiskers, Biomacromolecules 6 (2005) 1055–1061

[21] J. Huang, D. Rodrigue, Comparison of the mechanical properties between carbon nanotube and nanocrystalline cellulose polypropylene based nano-composites, Mater. Des. 65 (2015) 974–982

[22] E. Fortunati, D. Puglia, F. Luzi, C. Santulli, J.M. Kenny, L. Torre, Binary PVA bio-nanocomposites containing cellulose nanocrystals extracted from different natural sources: Part I, Carbohyd. Polym. 97 (2013) 825–836

[23] E. Fortunati, F. Luzi, D. Puglia, R. Petrucci, J.M. Kenny, L.Torre, Processing of PLA nanocomposites with cellulose nanocrystals extracted from Posidonia oceanica waste: Innovative reuse of coastal plant, Ind. Crop. Prod. 67 (2015) 439–447

[24] M.R. Kamal, V. Khoshkava, Effect of cellulose nanocrystals (CNC) on rheological and mechanical properties and crystallization behavior of PLA/CNC nanocomposites, Carbohyd. Polym. 123 (2015) 105–114

[25] M. Mariano, N. El Kissi, A. Dufresne, Cellulose nanocrystals and related nanocomposites: Review of some properties and challenges, J. Polym. Sci. Part B Polym. Phys. 52 (2014) 791–806

[26] K. Majeed, M. Jawaid, A. Hassan, A. Abu Bakar, H.P.S. Abdul Khalil, A.A Salema, I. Inuwa, Potential materials for food packaging from nanoclay/natural fibres filled hybrid composites, Mater. Des. 46 (2013) 391–410

[27] V. Ojijo, S.S. Ray, Processing strategies in bionanocomposites, Prog. Polym. Sci. 38 (2013) 1543–1589

[28] H. Bai, Y. Sun, J. Xu, W. Dong, X. Liu, Rheological and structural characterization of HA/PVA-SbQ composites film-forming solutions and resulting films as affected by UV irradiation time, Carbohyd. Polym. 115 (2015) 422–431

[29] C.H. Chen, W.S. Kuo, L.S. Lai, Rheological and physical characterization of film-forming solutions and edible films from tapioca starch/decolorized hsian-tsao leaf gum, Food. Hydrocolloid. 23 (2009) 2132–2140

[30] A. Silva-Weiss, V. Bifani, M. Ihl, P.J.A. Sobral, M.C. Gómez-Guillén, Polyphenol-rich extract from murta leaves on rheological properties of film-forming solutions based on different hydrocolloid blends, J. Food. Eng. 140 (2014) 28–38

[31] N. El Miri, M. El Achaby, A. Fihri, M. Larzek, M. Zahouily, K. Abdelouahdi, A. Barakat, A. Solhy, Synergistic effect of cellulose nanocrystals/graphene oxide nanosheets as functional hybrid nanofiller for enhancing properties of PVA nanocomposites, Carbohyd. Polym. 137 (2016) 239–248

[32] H.A. Silvério, W.P. Flauzino-Neto, N.O. Dantas, D. Pasquini, Extraction and characterization of cellulose nanocrystals from corncob for application as reinforcing agent in nanocomposites, Ind. Crop. Prod. 44 (2013) 427–436

[33] P. Lu, Y.L. Hsieh, Preparation and characterization of cellulose nanocrystals from rice straw, Carbohyd. Polym. 87 (2012) 564–573

[34] R.M. Dos Santos, W.P.F. Neto, H.A. Silvério, D.F. Martins, N.O. Dantas, D. Pasquini, Cellulose nanocrystals from pineapple leaf, a new approach for the reuse of this agro-waste, Ind. Crop. Prod. 50 (2013) 707–714

[35] E.d.M. Teixeira, T.J. Bondancia, K.B.R. Teodoro, A.C. Corrêa, J.M. Marconcini, L.H.C. Mattoso, Sugarcane bagasse whiskers: Extraction and characterizations, Ind. Crop. Prod. 33 (2011) 63–66

[36] S.J. Eichhorn, A. Dufresne, M. Aranguren, N.E. Marcovich, J.R. Capadona, S.J. Rowan, C. Weder, W. Thielemans, M. Roman, S. Renneckar, W. Gindl, S. Veigel, J. Keckes, H. Yano, K. Abe, M. Nogi, A.N. Nakagaito, A. Mangalam, J. Simonsen, A.S. Benight, A. Bismarck, L.A. Berglund, T. Peijs, Review: current international research into cellulose nanofibres and nanocomposites, J. Mater. Sci. 45 (2010) 1–33

[37] N.L. Garcia de Rodriguez, W. Thielemans, A. Dufresne, Sisal cellulose whiskers reinforced polyvinyl acetate nanocomposites, Cellulose 13 (2006) 261–270

[38] W.P.F. Flauzino-Neto, H.A. Silvério, N.O. Dantas, D. Pasquini, Extraction and characterization of cellulose nanocrystals from agro-industrial residue – Soy hulls, Ind. Crop. Prod. 42 (2013) 480–488

[39] D. Peressini, B. Bravin, R. Lapasin, C. Rizzotti, A. Sensidoni, Starch–methylcellulose based edible films: Rheological properties of film-forming dispersions , J. Food. Eng. 59 (2003) 25–32

[40] B. Cuq, C. Aymard, J.L. Cuq, S. Guilbert, Edible packaging films based on fish myofibrillar proteins: Formulation and functional properties, J. Food. Sci. 160 (1995) 1369–1374

[41] S.P. Rwei, S.W. Chen, C.F. Mao, H.W. Fang, Viscoelasticity and wearability of hyaluronate solutions, Biochem. Eng. J. 40 (2008) 211–217

[42] U. Florjancic, A. Zupancic, M. Zumer, Rheological characterization of aqueous polysaccharide mixtures undergoing shear, Chem. Biochem. Eng. Q. 16 (2002) 105–118.

[43] W.M. Kulicke, A.H. Kull, W. Kull, H. Thielking, Characterization of aqueous carboxymethylcellulose solutions in terms of their molecular structure and its influence on rheological behaviour, Polymer 37 (1996) 2723–2731

[44] C. Zhou, Q. Wang, Q. Wu, UV-initiated crosslinking of electrospun poly(ethylene oxide) nanofibers with pentaerythritol triacrylate: Effect of irradiation time and incorporated cellulose nanocrystals, Carbohyd. Polym. 87 (2012) 1779–1786

[45] D. Liu, X. Chen, Y. Yue, M. Chen, Q. Wu, Structure and rheology of nanocrystalline cellulose, Carbohyd. Polym. 84 (2011) 316–322

[46] A.H. Clark, S.B. Ross-Murphy, Structural and mechanical properties of biopolymer gels, Adv. Polym. Sci. 83 (1987) 57–192

[47] A.A. Oun, J.W. Rhim, Preparation and characterization of sodium carboxymethyl cellulose/cotton linter cellulose nanofibril composite films, Carbohyd. Polym. 127 (2015) 101–109

[48] J. Li, L. Shao, L. Yuan, Y. Wang, A novel strategy for making poly(vinyl alcohol)/reduced graphite oxide nanocomposites by solvothermal reduction, Mater. Des. 54 (2014) 520–525

[49] D. Hu, H. Wang, L. Wang, Physical properties and antibacterial activity of quaternized chitosan/carboxymethyl cellulose blend films, LWT Food Sci. Technol. 65 (2016) 398–405

[50] S.A. Paralikar, J. Simonsen, J. Lombardi, Poly(vinyl alcohol)/cellulose nanocrystal barrier membranes, J. Membr. Sci. 320 (2008) 248–258

[51] S. Mallakpour, A. Abdolmaleki, Z. khalesi, S. Borandeh, Surface functionalization of GO, preparation and characterization of PVA/TRIS-GO nanocomposites, Polymer 81 (2015) 140–150

[52] E. Fortunati, F. Luzi, A. Jiménez, D.A. Gopakumar, D. Puglia, S. Thomas, J.M. Kenny, A. Chiralt, L. Torre, Revalorization of sunflower stalks as novel sources of cellulose nanofibrils and nanocrystals and their effect on wheat gluten bionanocomposite properties, Carbohyd. Polym. 149 (2016) 357–368

[53] H. Yu, B. Sun, D. Zhang, G. Chen, X. Yang, J. Yao, Reinforcement of biodegradable poly(3-hydroxybutyrate-co-3-hydroxyvalerate) with cellulose nanocrystal/silver nanohybrids as bifunctional nanofillers, J. Mater. Chem. B. 2 (2014) 8479–8489

[54] R. S. Kanatt, M.S. Rao, S.P. Chawla, Arun Sharma, Active chitosane polyvinyl alcohol films with natural extracts, Food. Hydrocolloid. 29 (2012) 290–297

[55] J. Bonilla, E. Fortunati, L. Atarés, A. Chiralt, J.M. Kenny, Physical structural and antimicrobial properties of poly vinyl alcohol chitosan biodegradable films, Food. Hydrocolloid. 35 (2014) 463–470

[56] X. Hu, T. Wang, L. Xiong, C. Wang, X. Liu, Z. Tong, Preferential adsorption of poly(ethylene glycol) on hectorite clay and effects on poly(N-isopropylacrylamide)/hectorite nanocomposite hydrogels, Langmuir 26 (6) 2010 4233–4238

[57] X. Hu, L. Xiong, T. Wang, Z. Lin, X. Liu, Z.Tong, Synthesis and dual response of ionic nanocomposite hydrogels with ultrahigh tensibility and transparence, Polymer 50 (2009) 1933–1938

[58] H. Almasi, B. Ghanbarzadeh, A.A. Entezami, Physicochemical properties of starch–CMC–nanoclay biodegradable films, Int. J. Biol. Macromol. 46 (2010) 1–5

[59] K.M.Z. Hossain, I. Ahmed, A.J. Parsons, C.A. Scotchford, G.S. Walker, W. Thielemans, C.D. Rudd, Physico-chemical and mechanical properties of nanocomposites prepared using cellulose nanowhiskers and poly(lactic acid), J. Mater. Sci. 47 (2012) 2675–2686.

[60] R. Arjmandi, A. Hassan, S.J. Eichhorn, M.K. Mohamad Haafiz, Z. Zakaria, F.A. Tanjung, Enhanced ductility and tensile properties of hybrid montmorillonite/cellulose nanowhiskers reinforced polylactic acid nanocomposites, J. Mater. Sci. 50 (2015) 3118–3130